Reduction Kinetics of the Ferredoxin–Ferredoxin-NADP$^+$ Reductase Complex: A Laser Flash Photolysis Study†

Anjan K. Bhattacharyya, Terrance E. Meyer, and Gordon Tollin*
Department of Biochemistry, University of Arizona, Tucson, Arizona 85721
Received September 9, 1985; Revised Manuscript Received December 3, 1985

ABSTRACT: The kinetics of reduction of spinach ferredoxin (Fd), ferredoxin-NADP$^+$ reductase (FNR), and the Fd–FNR complex have been investigated by the laser flash photolysis technique. 5-Deazariboflavin semiquinone (5-dRf$^\bullet$), generated in situ by laser flash photolysis under anaerobic conditions, rapidly reduced both oxidized Fd (Fd_{ox}) ($k = 2 \times 10^8$ M^{-1} s^{-1}) and oxidized FNR (FNR_{ox}) ($k = 6.3 \times 10^8$ M^{-1} s^{-1}) at low ionic strength (10 mM) at pH 7.0, leading to the formation of reduced Fd (Fd_{red}) and FNR semiquinone (FNR$^\bullet$), respectively. At higher ionic strengths (310 and 460 mM), the rate constant for the reduction of the free Fd_{ox} increased about 3-fold ($k = 6.7 \times 10^8$ M^{-1} s^{-1} at 310 mM and 6.4×10^8 M^{-1} s^{-1} at 460 mM). No change in the second-order rate constant for reduction of the free FNR_{ox} was observed at high ionic strength. At low ionic strength (10 mM), 5-dRf$^\bullet$ reacted only with the FAD center of the preformed 1:1 Fd_{ox}–FNR_{ox} complex ($k = 5.6 \times 10^8$ M^{-1} s^{-1}), leading to the formation of FNR$^\bullet$. No direct reduction of Fd_{ox} in the complex was observed. No change in the kinetics occurred in the presence of excess NADP$^+$. The second-order rate constant for reduction of Fd_{ox} by 5-dRf$^\bullet$ in the presence of a stoichiometric amount of fully reduced FNR at low ionic strength was 7×10^6 M^{-1} s^{-1}, i.e., about one-thirtieth the rate constant for reduction of free Fd_{ox}. Thus, the iron–sulfur center is sterically hindered in the complex, whereas the FAD is not. The reoxidation of Fd_{red} by low concentrations of FNR_{ox} at pH 7.0 and high ionic strength (310 mM) was observed to be second order ($k = 1.5 \times 10^8$ M^{-1} s^{-1}). At high FNR_{ox} concentrations, saturation was observed, and a limiting first-order rate constant of 4000 s^{-1} was obtained, corresponding to electron transfer occurring within a transient Fd_{red}–FNR_{ox} complex. Inclusion of excess NADP$^+$ did not alter the observed kinetics. Increasing the ionic strength to 460 mM resulted in a decrease in both the second-order rate constant and the limiting first-order rate constant (7×10^7 M^{-1} s^{-1} and 1600 s^{-1}, respectively). This is presumably due to electrostatic interactions between complementary negative charges on Fd and positive charges on FNR. At pH 6.0 at high ionic strength (310 mM), the reaction of Fd_{red} with FNR_{ox} was second order, and saturation was not observed ($k = 3.0 \times 10^8$ M^{-1} s^{-1}). At higher ionic strength (460 mM), however, the second-order rate constant decreased ($k = 1.3 \times 10^8$ M^{-1} s^{-1}), and saturation was observed at high FNR_{ox} concentrations. A limiting first-order rate constant of 3400 s^{-1} was obtained. No reoxidation of Fd_{red} was detectable at pH 8.0 at high ionic strength (310 mM). These results are consistent with the expected pH dependence of the difference in redox potential between Fd_{ox} and FNR_{ox}. The effect of ionic strength on the first-order rate constant suggests the formation of nonoptimal complexes, which have variation in the orientation and/or the distance between the FAD and iron–sulfur centers within the complex.

In order to obtain a better understanding of biological electron-transfer reactions occurring within protein–protein complexes, we have been investigating the reduction kinetics of several physiological and nonphysiological multicomponent water-soluble redox systems (Przysiecki et al., 1985; Ahmad et al., 1982; Simondsen et al., 1982; Simondsen & Tollin, 1983; Hazzard & Tollin, 1985; Hazzard et al., 1986). Our primary goal is to identify specific factors that control the observed rate constants of electron transfer to and between the components of these systems. Possible controlling factors include the difference in redox potential between participating electron carriers, distances, relative orientations, and degrees of solvent exposure of redox centers, site-specific and overall charge distributions, etc. This work has centered mainly on electrostatic complexes formed between redox proteins of opposite net charge. In a previous paper (Przysiecki et al., 1985), we described the kinetics of electron transfer between spinach ferredoxin-NADP$^+$ reductase (FNR)[1] and the nonphysiological electron acceptor *Clostridium pasteurianum* rubredoxin. More recently, we have studied complex formation and the kinetics of electron transfer between spinach FNR and several other nonphysiological acidic iron-containing redox proteins (Bhattacharyya et al., 1986). In the present paper, we report an extension of this work to the redox kinetics of the physiological spinach Fd–FNR system.

These latter two proteins are directly involved in the terminal steps of photosynthetic electron transfer leading to the formation of reduced NADP$^+$. Fd_{ox} accepts electrons from the reducing end of photosystem I, and transfers electrons to NADP$^+$ via FNR, by a mechanism probably involving two one-electron steps. At low ionic strength, Fd_{ox} and FNR_{ox} have been shown to form a 1:1 electrostatically stabilized complex, which decreases in stability with increasing ionic strength (Batie & Kamin, 1981, 1984a,b; Shin et al., 1982; Knaff et al., 1980; Smith et al., 1981a,b). The main purpose of the present study was to investigate the electron-transfer properties

† Supported in part by National Institutes of Health Grants AM15057 and GM21277.

[1] Abbreviations: Fd_{ox}, oxidized ferredoxin; Fd_{red}, reduced ferredoxin; FNR, ferredoxin-NADP$^+$ reductase; FNR_{ox}, oxidized ferredoxin-NADP$^+$ reductase; FNR$^\bullet$, ferredoxin-NADP$^+$ reductase neutral semiquinone; FNR_{red}, fully reduced ferredoxin-NADP$^+$ reductase; 5-dRf, 5-deazariboflavin; 5-dRf$^\bullet$, 5-deazariboflavin semiquinone; Bistrispropane, 1,3-bis[[tris(hydroxymethyl)methyl]amino]propane.

0006-2960/86/0425-4655$01.50/0

of the individual components and their complex at low and high ionic strengths, in an attempt to obtain the rate constant for intramolecular one-electron transfer from reduced ferredoxin to oxidized FNR and to explore the accessibility of the protein redox centers within the complex.

Although a moderate amount of information is currently available concerning complex formation between these two proteins, little is known about electron-transfer kinetics, partly as a consequence of the low redox potentials of the proteins and because of the rapidity of the intermolecular electron-transfer reaction. Pulse radiolysis studies of the 1:1 complex using the $NADP^+$ radical as the reactant have shown that only direct reduction of the FAD center in FNR occurs at low ionic strength (Maskiewicz & Bielski, 1982). Batie and Kamin and others (Batie and Kamin, 1984a,b; Masaki et al., 1982), using stopped-flow techniques, have reported that the one-electron transfer from Fd_{red} to FNR_{ox} leading to formation of the FNR semiquinone occurred within the dead time of the apparatus (less than 2 ms) at low ionic strength, whereas the reduction of FNR• to FNR_{red} occurred at a much slower rate (37–80 s^{-1}).

In order to reduce the proteins using nonmixing techniques, we have employed laser flash photolysis of free flavins to generate a reductant under anaerobic conditions. This method permits the rapid in situ generation (<1 μs) of a very strong reductant (flavosemiquinone) and thus allows the measurement of reactions that are too fast to be followed by conventional mixing techniques. We have previously demonstrated the utility of this method in measuring rates of electron-transfer reactions in several systems (Bhattacharyya et al., 1983, 1985; Cusanovich & Tollin, 1980; Tollin et al., 1982; Cusanovich et al., 1985). In the current study, we have investigated the electron-transfer properties of the individual components and their 1:1 mixture at different ionic strengths and pH values and have successfully measured the limiting first-order rate constant for electron transfer from Fd_{red} to FNR_{ox} at pH 7 and high ionic strength. Because of the low redox potentials of Fd and FNR (Fd, $E_{m,7}$ = –420 mV; FNR, $E_{m,7}$ = –320 mV) (Stombaugh et al., 1976; Keirns & Wang, 1972), we utilized the semiquinone of 5-deazariboflavin ($E_{m,7}$ = –650 mV) (Blankenhorn, 1976) as the reductant.

Materials and Methods

Spinach FNR and Fd were purified according to the method of Zanetti and Curti (1980). A few experiments were performed with FNR that was a kind gift from Dr. E. Gross. Extinction coefficients of 10.3×10^3 and 9.7×10^3 M^{-1} cm^{-1} at 458 and 420 nm (Foust et al., 1969) were used to determine the concentrations of oxidized FNR and Fd, respectively. All buffer components were ACS-reagent grade. The buffer used for the low ionic strength experiments at pH 6.0 and 7.0 was 4 mM potassium phosphate–0.5 mM ethylenediaminetetraacetic acid (EDTA) and ~100 μM 5-dRf (I = 10 mM). At pH 8.0, 10 mM Bistrispropane–0.5 mM EDTA buffer was used. Potassium chloride was used to adjust buffer solutions to the appropriate ionic strengths.

All kinetic experiments were performed under pseudo-first-order conditions, in which the concentration of oxidized protein was in large excess over the amount of 5-dRf• produced per flash (<0.7 μM). Unless quantitation was required (e.g., for flash-induced difference spectra) the number of flashes per kinetic trace varied. Furthermore, in the presence of increasing amounts of oxidized protein, due to absorbance of the exciting laser light, the amount of 5-dRf• produced per flash was diminished. All kinetic traces were analyzed by hand, by fitting to an exponential curve. All kinetic experiments were carried out at room temperature (23–25 °C) under anaerobic conditions. Although the photochemical reaction that generates 5-dRf• also produces a radical species derived from EDTA, in this study as in all of our previous work, no kinetic complications have been observed during the initial phase of protein reduction which could be attributed to this material or to any reaction products derived from it. Thus, exponentiality was maintained within experimental error. As will be shown later, in some experimental situations slower absorbance changes were obtained that could in principle arise from this source. However, the kinetic behavior of these transients (i.e., independence of protein concentration) and the time-resolved difference spectral properties were inconsistent with such an explanation. A description of the laser flash apparatus and the method of data collection and analysis has been published elsewhere (Przysiecki et al., 1985; Bhattacharyya et al., 1983).

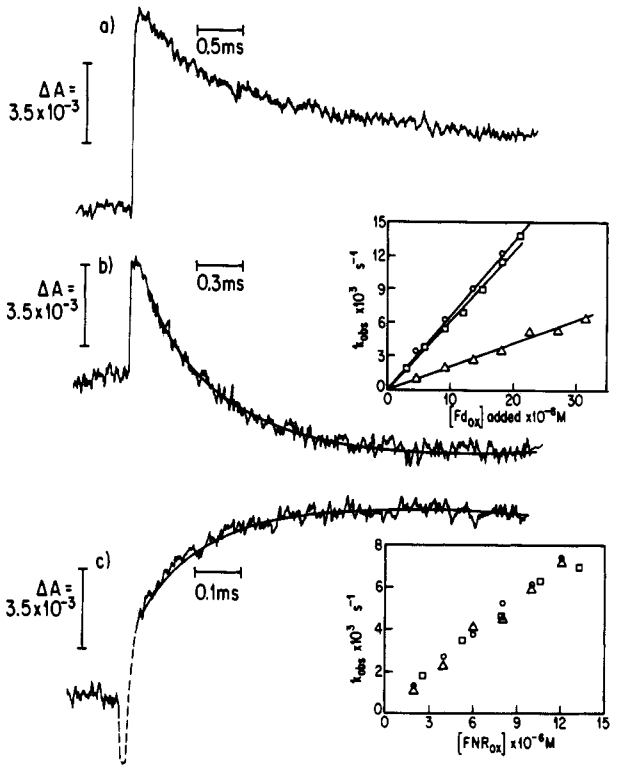

FIGURE 1: Kinetic traces representing the following: (a) Rapid formation and slower disproportionation of 5-dRf• in the absence of Fd_{ox} and FNR_{ox} at I = 10 mM, pH 7. (b) Reduction of Fd_{ox} monitored at 500 nm. Buffer conditions as in (a). The protein concentration was 9 μM. The inset shows second-order plots of k_{obsd} vs. Fd_{ox} concentration at (Δ) 10, (○) 310, and (□) 460 mM ionic strengths. (c) Formation of FNR• monitored at 590 nm. FNR_{ox} concentration was 11 μM. The initial rapid rise (dashed line) corresponds to a scattering artifact. However, the exponential portion of the trace extrapolates to the preflash base line at zero time. The inset shows second-order plots of k_{obsd} vs. FNR_{ox} concentration at ionic strengths of (○) 10 and (Δ) 310 mM and (□) a 1:1 Fd_{ox}–FNR_{ox} mixture at I = 10 mM. Solid lines in (b) and (c) are single-exponential curves drawn through the data.

Results and Discussion

Kinetics of Reduction of Individual Proteins. The laser-induced kinetic trace shown in Figure 1a illustrates the rapid formation (<2 μs) and slower disproportionation of 5-dRf• that occurred in the absence of oxidized protein, as monitored at 500 nm. The process can be represented by the equation:

$$5\text{-dRf}_{ox} + e^- \xrightarrow[H^+]{h\nu} 5\text{-dRfH}\cdot \xrightarrow[5\text{-dRfH}\cdot]{} 5\text{-dRf}_{ox} + 5\text{-dRfH}_2$$

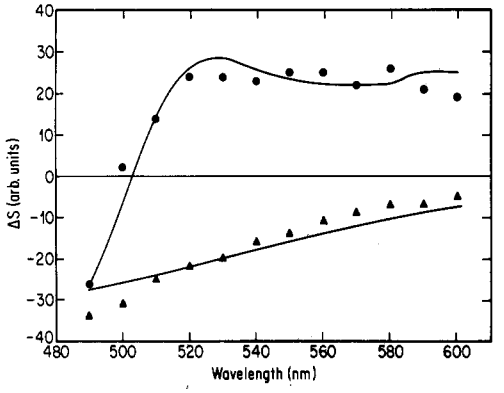

FIGURE 2: (▲) Laser flash induced difference spectrum corresponding to Fd_{ox} reduction by 5-dRf$^\bullet$ measured 5 ms following the laser flash at I = 10 mM, pH = 7, for 22 μM free Fd_{ox}. The solid line represents the dithionite-reduced Fd_{red} minus Fd_{ox} spectrum obtained in a spectrophotometer. The spectral data were normalized to the flash data at 520 nm. (●) Laser flash induced difference spectrum corresponding to reduction of FNR_{ox} to FNR$^\bullet$ by 5-dRf$^\bullet$, measured 600 ms following the laser flash, for 11 μM free FNR_{ox}. The solid line corresponds to the FNR$^\bullet$ minus FNR_{ox} spectrum obtained by steady-state photoreduction in a spectrophotometer. The spectral data were normalized to the flash data at 570 nm.

Table I: Second-Order Rate Constants Corresponding to Reaction between 5-dRf$^\bullet$, Fd_{ox}, and FNR_{ox} at pH 7 and Various Ionic Strengths

protein	ionic strength (mM)	$k_2 \times 10^8$ M^{-1} s^{-1}
Fd_{ox}	10	2.0
	310	6.7
	460	6.4
FNR_{ox}	10	6.3
	310	5.9
Fd_{ox}–FNR_{ox}	10	5.6
Fd_{ox}–FNR_{red}	10	0.07

In the presence of Fd_{ox} at 10 mM ionic strength (Figure 1b), laser photolysis resulted in an initial increase in absorbance at 500 nm,[2] followed by an exponential decay that eventually went below the preflash base line. Such changes are consistent with the rapid formation of 5-dRf$^\bullet$ and its subsequent reoxidation by Fd_{ox}, leading to formation of Fd_{red}. Under these conditions, 5-dRf$^\bullet$ disproportionation no longer occurred because virtually all of the deazaflavin radical had reacted with the oxidized protein.[3] The flash-induced difference spectrum obtained by similar measurements as a function of wavelength, monitored 5 ms following the laser flash, was consistent with this interpretation (solid triangles, Figure 2; on this time scale all kinetic processes were complete). The solid line through the points in Figure 2 represents a Fd_{red} minus Fd_{ox} difference spectrum obtained by dithionite reduction of Fd_{ox} in a spectrophotometer. As is evident, the agreement is satisfactory. From a plot of k_{obsd} vs. Fd_{ox} concentration, a second-order rate constant for the reduction of Fd_{ox} by dRf$^\bullet$ of 2.0×10^8 M^{-1} s^{-1} was obtained (inset, Figure 1b; Table I). At higher ionic strengths (310 and 460 mM) and at pH 7.0, the second-order rate constant for the above-mentioned reaction increased approximately 3-fold (6.7×10^8 M^{-1} s^{-1} and 6.4×10^8 M^{-1} s^{-1} at 310 and 460 mM, respectively; inset, Figure 1b; Table I). This increase in rate constant at the high ionic strengths could be a result of a salt-induced conformational change or a change in redox potential of Fd_{ox}. This deserves further investigation.

[2] This is an apparent FNR_{ox}/FNR$^\bullet$ isosbestic wavelength when the present optical system is used.

[3] At lower protein concentrations, mixed kinetics were observed corresponding to the simultaneous occurrence of both disproportionation and protein reduction. This was easily recognized, however, and rate constant determinations were usually carried out at protein concentrations that were high enough to avoid this problem.

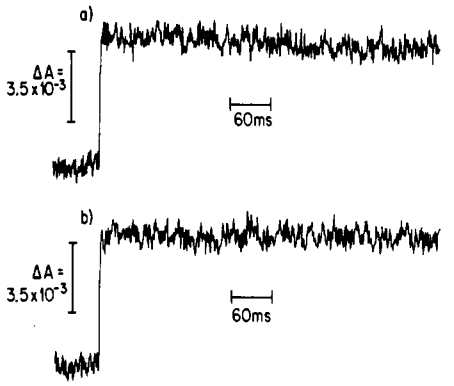

FIGURE 3: Kinetic traces demonstrating stability of FNR$^\bullet$ monitored at 590 nm. (a) 11 μM FNR_{ox} and (b) 14 μM 1:1 Fd_{ox}–FNR_{ox}, both at I = 10 mM, pH 7.

The reaction of 5-dRf$^\bullet$ with FNR_{ox} at I = 10 mM was followed as an exponential increase in absorbance at 590 nm (Figure 1c). The product was kinetically stable up to 600 ms following the laser flash (Figure 3a). The flash-induced difference spectrum (solid circles, Figure 2) is consistent with formation of the FNR neutral (blue) semiquinone (FNR$^\bullet$). The corresponding solid line through the data points in Figure 2 represents the FNR$^\bullet$ minus FNR_{ox} difference spectrum obtained by steady-state photoreduction in a spectrophotometer. Again, the agreement is satisfactory. The second-order rate constant corresponding to the reaction of 5-dRf$^\bullet$ with FNR_{ox} was 6.3×10^8 M^{-1} s^{-1} at I = 10 mM, pH 7.0 (inset, Figure 1c; Table I). No significant change in the second-order rate constant could be detected at I = 310 mM, pH 7.0 (inset, Figure 1c; Table I).

Kinetics of Reduction of the 1:1 Complex at Low Ionic Strength. On the basis of the reported redox potentials of Fd and FNR (Keirns & Wang, 1972; Batie & Kamin, 1981; Smith et al., 1981a,b), it is expected that the predominant direction of intracomplex electron transfer at pH 7.0 would involve a reaction between Fd_{red} and FNR_{ox} leading to the formation of FNR$^\bullet$ (>10:1). As shown earlier, however, at I = 10 mM and pH 7.0 the rate constants for reduction of the isolated proteins by 5-dRf$^\bullet$ would favor an initial reduction of FNR upon laser photolysis (~3-fold, 6.3×10^8 vs. 2×10^8 M^{-1} s^{-1}). In order to directly determine the sequence of events upon 5-dRf$^\bullet$ interaction with the complex, we added increasing amounts of a 1:1 Fd_{ox}–FNR_{ox} solution to a low ionic strength buffer (10 mM, pH 7.0) containing 5-dRf. Upon flash photolysis, no direct reduction of Fd_{ox} was observed (at the FNR isosbestic point of 500 nm). However, we were able to observe direct reduction of the FAD center of FNR, leading to the formation of FNR$^\bullet$, which was kinetically stable up to at least 600 ms following the laser flash (Figure 3b). The flash-induced difference spectrum obtained was similar to that observed for free FNR (data not shown). A plot of k_{obsd} vs. complex concentration yielded a second-order rate constant of 5.6×10^8 M^{-1} s^{-1} for electron transfer from 5-dRf$^\bullet$ to the FAD in the oxidized Fd–FNR complex (inset, Figure 1c; Table I), almost the same as for the isolated FNR. These observations demonstrate that upon complexation the FAD center in FNR remains as accessible to reduction by 5-dRf$^\bullet$ as it was in the free state. Inclusion of an excess of $NADP^+$ (~6-fold) into the reaction mixture did not alter the kinetics of reduction of the complex at low ionic strength (data not shown).

To further investigate the reactivity of the iron–sulfur center of Fd in the complex, we performed laser photolysis experi-

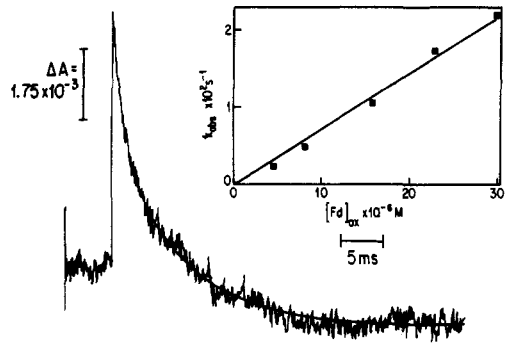

FIGURE 4: Kinetic trace representing the slow reduction of 14 μM Fd_{ox} in the presence of a stoichiometric amount of FNR_{red}, monitored at 500 nm. The solid line is an exponential curve drawn through the data. The inset shows a second-order plot of k_{obsd} vs. Fd_{ox} concentration in the presence of stoichiometric amounts of FNR_{red}, at I = 10 mM, pH 7.0.

ments in the presence of a stoichiometric amount of fully reduced FNR at low ionic strength (10 mM). Upon flash photolysis, after its initial rapid formation, 5-dRf$^{\bullet}$ was found to react with Fd_{ox} with a rate constant approximately one-thirtieth that of uncomplexed Fd_{ox}. The kinetic trace shown in Figure 4 represents the slow reduction of Fd_{ox} by 5-dRf$^{\bullet}$ in the semireduced complex. If the slow process represented dissociation of the semireduced complex, the observed kinetics would be independent of concentration (i.e., first order). This was not the case, however. A plot of k_{obsd} vs. complex concentration (expressed as Fd_{ox} added; Figure 4, inset; Table I) yielded a second-order rate constant of 7×10^6 M^{-1} s^{-1}. The flash-induced difference spectrum was consistent with formation of Fd_{red} (data not shown). These results indicate that access to the 2Fe-2S center is partially blocked upon complexation.[4] This is consistent with the above-mentioned results of Maskiewicz and Bielski (1982) and with EPR experiments in which Dy^{3+} was used as a paramagnetic probe to determine the degree of exposure of the iron–sulfur and FAD centers of the partially reduced Fd–FNR complex (Batie & Kamin, 1984a,b). In these experiments the extent of line broadening of the signal corresponding to the reduced 2Fe-2S center was significantly decreased upon addition of a stoichiometric amount of FNR_{red} at low ionic strength. This result suggests that complex formation occurs between Fd_{red} and FNR_{red} at low ionic strength and that the accessibility of the 2Fe-2S center to Dy^{3+} is diminished upon complex formation.

Kinetics of Reduction of Protein Mixtures at High Ionic Strength. As noted above, the reaction between Fd_{red} and FNR_{ox}, leading to FNR$^{\bullet}$ formation, has been found to occur in the dead time of the stopped-flow instrument. In an attempt to directly observe 5-dRf$^{\bullet}$ reduction of Fd_{ox} and subsequent reoxidation of Fd_{red}, we added increasing amounts of FNR_{ox} to a high ionic strength solution (310 mM) at pH 7.0 containing Fd_{ox} and 5-dRf. Upon flash photolysis, monitored at 500 nm, an initial decrease in absorbance was observed, followed by an exponential increase (Figure 5a). This is consistent with the rapid formation[5] and slower reoxidation of Fd_{red}. In the absence of FNR, no reoxidation of Fd_{red} occurred on the same time scale (data not shown). Furthermore, when

[4] The relatively small change in redox potential that occurs upon complex formation (Batie & Kamin, 1981) is not sufficient to account for such a large change in rate constant [cf. Meyer et al. (1983)].

[5] Due to the overlap between the kinetics of fast reduction of Fd_{ox} and the reoxidation of Fd_{red}, an exact value for the second-order rate constant for reduction of Fd_{ox} in the faster reaction could not be accurately determined.

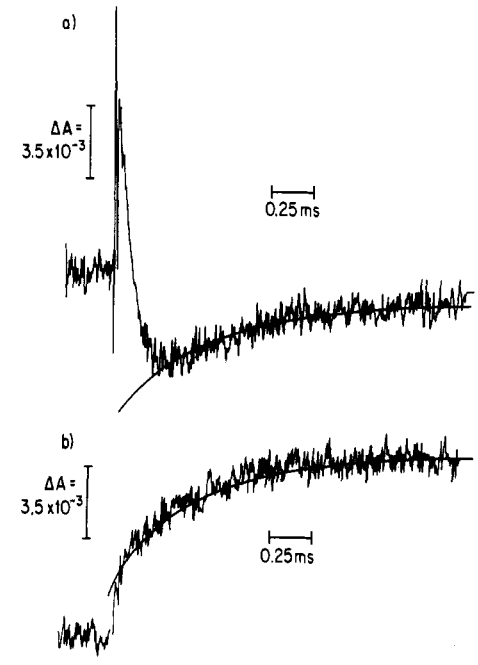

FIGURE 5: Kinetic traces showing (a) formation of Fd_{red} followed by its subsequent reoxidation by FNR_{ox} monitored at 500 nm and (b) reduction of FNR_{ox} to FNR$^{\bullet}$ by Fd_{red}, monitored at 590 nm. I = 310 mM, pH 7. Concentrations of Fd_{ox} and FNR_{ox} were 15 and 14 μM, respectively. The solid lines are exponential curves drawn through the data.

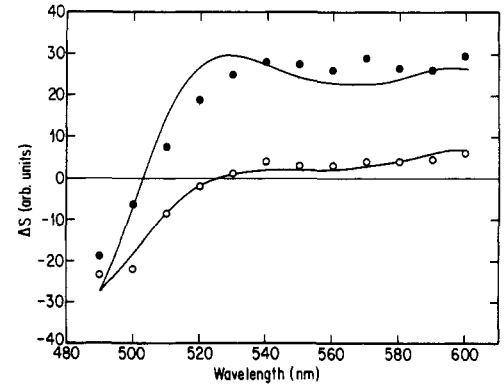

FIGURE 6: Laser flash induced difference spectra corresponding to the reactions described in Figure 5. (○) t = 0 ms and (●) t = 2.5 ms. Protein concentrations and buffer conditions were as described in Figure 5. The solid line drawn through the data represented by (●) was obtained as described in Figure 2. The solid line drawn through the data represented by (○) corresponds to the sum of the difference spectra of equal concentrations of Fd_{red} and FNR$^{\bullet}$.

this same experiment was carried out at low ionic strength (10 mM), i.e., under conditions in which FNR would be complexed, again no reoxidation of Fd_{red} was observed (data not shown). This latter result is consistent with the lack of reduction of complexed Fd described in the previous section. With increasing FNR_{ox} concentrations at 310 mM ionic strength, the amount of free Fd_{ox} reduced directly by 5-dRf$^{\bullet}$ progressively decreased, while the amount of FNR$^{\bullet}$ formed increased. The formation of FNR$^{\bullet}$ was followed by the absorbance increase at 590 nm (where Fd_{red} reoxidation would also result in an increase in absorbance) (Figure 5b). As the FNR_{ox} concentration was increased, the rate of reoxidation of Fd_{red} increased, as did the rate of formation of FNR$^{\bullet}$ (monitored at 590 nm). The time-resolved flash-induced difference spectra monitored at t = 0 ms (extrapolated) and t = 2.5 ms (when all kinetic processes were complete) (Figure 6) are consistent with electron transfer from Fd_{red} to FNR_{ox}.

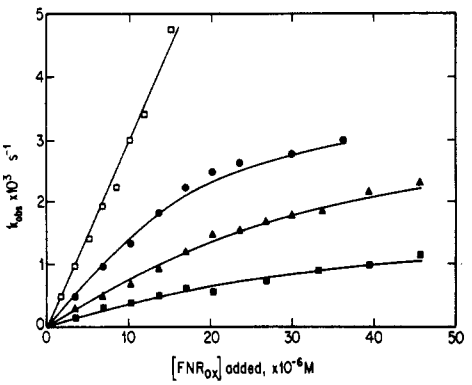

FIGURE 7: Plots of k_{obsd} vs. FNR_{ox} concentration for Fd_{red} reoxidation at different pH and ionic strengths: (□) pH 6, I = 310 mM; (▲) pH 6, I = 460 mM; (●) pH 7, I = 310 mM; (■) pH 7, I = 460 mM. The initial Fd_{ox} concentration in all cases was 15.5 μM. Solid curves correspond to theoretical fits to the two-step mechanism given in the text.

Table II: Effect of pH and Ionic Strength on the Rate Constants for the Electron-Transfer Reaction between Fd_{red} and FNR_{ox}

pH	ionic strength (mM)	k_{12} (M^{-1} s^{-1})	k_{21} (s^{-1})	k_{23} (s^{-1})
7.0	310	1.5×10^8	1.9×10^3	4.0×10^3
7.0	460	7.0×10^7	1.3×10^3	1.6×10^3
6.0	310	3.0×10^8		$(7.0 \times 10^3)^a$
6.0	460	1.3×10^8	2.2×10^3	3.4×10^3

[a] This value is an estimate (see text for details).

The small positive signal observed at t = 0 ms (extrapolation of exponential curve to zero time in Figure 5b) corresponds to direct reduction of FNR_{ox} by 5-dRf$^\bullet$. The solid line drawn through the flash data given by the closed circles in Figure 6 represents an FNR$^\bullet$ minus FNR_{ox} spectrum obtained by the steady-state photoreduction of FNR_{ox} in a spectrophotometer. It is evident that the agreement is good. The line drawn through the data represented by the open circles corresponds to the sum of the difference spectra of FNR$^\bullet$ and Fd_{red} and represents the initial direct reduction of approximately equal amounts of both FNR_{ox} and Fd_{ox} by 5-dRf$^\bullet$ (see legend to Figure 6 for details). Once again the agreement is satisfactory. At t = 2.5 ms then, essentially all of the Fd_{red} formed by the reaction of Fd_{ox} with 5-dRf$^\bullet$ had reacted with FNR_{ox} to produce FNR$^\bullet$.

At low FNR_{ox} concentrations, second-order kinetics were observed for this electron-transfer reaction from Fd_{red} to FNR_{ox}, whereas at higher FNR_{ox} concentrations (ratio of $FNR_{ox}/Fd_{ox} > 1.0$) the k_{obsd} values became relatively independent of protein concentration (Figure 7). The individual rate constants were obtained by a least-squares fit of the data to a simple two-step mechanism, in which the reactants form a transient complex followed by intracomplex electron transfer and product formation. This may be represented as

$$Fd_{red} + FNR_{ox} \underset{k_{21}}{\overset{k_{12}}{\rightleftharpoons}} (Fd_{red}\cdots FNR_{ox}) \underset{k_{32}}{\overset{k_{23}}{\rightleftharpoons}} Fd_{ox} + FNR^\bullet$$

Data fits that included k_{32} (the rate constant for reverse electron transfer from FNR$^\bullet$ to Fd_{ox}) did not appreciably alter the values obtained for the other rate constants (listed in Table II); a maximal value of ~100 s^{-1} was obtained for k_{32}. The solid lines in Figure 7 are the theoretical fits. As is evident, the agreement is quite good. On the basis of the extent of reoxidation of Fd_{red} observed at low FNR_{ox} concentrations (30–35%), a redox potential difference (at I = 310 mM, pH 7.0) of approximately 50 mV can be calculated between the one-electron-reduced Fd and FNR (see below). When the same experiment was carried out in the presence of excess $NADP^+$ (~6-fold), essentially no change in the kinetics was observed (data not shown).

Ionic strength effects are expected to occur on the second-order rate constant for this reaction, due to electrostatic interactions between the positively and negatively charged sites on FNR and Fd, respectively, and are not expected to be manifested on the limiting first-order rate constant unless the k_{23} step contains a contribution from any rearrangement or reorientation of the two redox proteins during nonoptimal collisions that might occur prior to formation of the actual electron-transfer complex (Simondsen & Tollin, 1983). In order to investigate this further, a similar experiment was performed at pH 7.0 and at an ionic strength of 460 mM. Upon flash photolysis under these conditions, the second-order rate constant for reoxidation of Fd_{red} in the presence of FNR_{ox} decreased, as did the limiting first-order rate constant (Table II; see also Figure 7). These ionic strength effects are consistent with a plus–minus (attractive) interaction between the two proteins and demonstrate that electrostatics play an important role in the formation of a productive electron-transfer complex. This suggests that the attractive force between the two components acts to optimize the mutual orientation between the redox centers for electron transfer. This also accounts for the similar ionic strength effects on the second- and first-order rate constants (cf. Table II). Thus, at higher ionic strengths there will be a greater probability of unfavorable orientations upon collision than at lower ionic strengths, which will act to slow the subsequent product formation step. These results are similar to those observed for the flavodoxin–cytochrome c complex (Simondsen et al., 1982, Simondsen & Tollin, 1983, Matthew et al., 1983, Weber & Tollin, 1985).

In order to study the effect of pH on the rate constant for electron transfer between Fd_{red} and FNR_{ox}, the same experiment was performed at two other pH values (pH 6.0 and 8.0). The rationale behind these experiments is that since the redox potential of Fd changes only slightly with pH [~3–4 mV/pH unit (Stombaugh et al., 1976)] and the one-electron $\Delta E/\Delta$pH of free flavins and a number of flavoproteins[6] varies by ~60 mV/pH unit (Stankovich et al., 1978; Ohnishi et al., 1981; Mayhew et al., 1969; Draper & Ingraham, 1968; O'Donnell & Williams, 1983), one would expect the FNR potential to become more negative as the pH is raised above 6.0 and to approach the Fd potential which remains essentially the same. Any pH-induced changes in the redox potential difference between Fd and FNR should then be reflected in the electron-transfer rate constant (Meyer et al., 1983). At pH 6.0, I = 310 mM, the reaction between Fd_{red} and FNR_{ox} was second order ($k = 3.0 \times 10^8$ M^{-1} s^{-1}), and no saturation kinetics were observed over the accessible concentration range (Figure 7; Table II). However, the larger second-order rate constant is consistent with the expected greater potential difference between Fd and FNR at pH 6.0 Since the effect of ionic strength at pH 7.0 was to decrease both the second-order and the limiting rate constants, we investigated the electron transfer kinetics at pH 6.0 and I = 460 mM in an attempt to determine if saturation kinetics could be observed. As in the case of the pH 7.0 experiment, the second-order rate

[6] The dependence of redox potential on pH has not been determined for FNR. However, literature values of −430 mV at pH 8 and −320 mV at pH 7 (Batie & Kamin, 1984; Keirns & Wang, 1972) for the one-electron potential of FNR give a larger than expected potential difference for this pH range but are consistent with an increase in redox potential with decreasing pH.

constant decreased ($k = 1.3 \times 10^8$ M^{-1} s^{-1}), and saturation was observed at high FNR_{ox} concentrations (Figure 7). The limiting first-order rate constant had a value of 3.4×10^3 s^{-1} (Table II).

The second-order rate constants at both pH 7.0 and 6.0 decreased approximately 2-fold when the ionic strength was increased from 310 to 460 mM. In the case of the limiting first-order rate constant, the decrease was also approximately 2-fold at pH 7.0. It is thus possible to estimate a value for the limiting rate constant of $\sim$7000 s^{-1} at pH 6.0 and 310 mM (Table II).

The kinetics of Fd_{red} decay were also investigated at pH 8.0 and high ionic strength. Under these conditions, no reoxidation of Fd_{red} in the presence of FNR_{ox} could be detected (data not shown). This result is inconsistent with the reported redox potentials for Fd_{ox}/Fd_{red} ($E_m \sim -420$ mV) and $FNR_{ox}/FNR^{\bullet}$ ($E_m \sim -430$ mV) (Batie & Kamin, 1984a,b) at pH 8.0 in that one would expect approximately equal distribution of electrons between the two reduced species and thus to observe some reoxidation of Fd_{red} under these conditions. This result suggests that the reported literature value for the one-electron potential of FNR at pH 8 may be incorrect. However, it is consistent with the 50-mV difference in redox potentials calculated at pH 7.0 (Fd > FNR). Another possibility is that the redox potential for Fd has changed from the reported value as a result of the high ionic strength. This needs further investigation.

Conclusions

The results reported above constitute a direct observation of rapid electron transfer between Fd_{red} and FNR_{ox} within a transient electron-transfer complex leading to the formation of $FNR^{\bullet}$. The values (cf. Table II) obtained for the intracomplex electron-transfer rate constant ($>1.6 \times 10^3$ s^{-1}) are consistent with the reaction being too rapid to observe with stopped-flow methods. The magnitude of the second-order rate constants observed at pH 6.0 and 7.0 and the existence and direction of ionic strength effects indicate that the reaction between the two proteins is strongly influenced by complementary electrostatic charges on the protein surfaces and is close to being diffusion controlled. The effects of pH on the rate constants are consistent with previous results (Meyer et al., 1983) that demonstrate a relationship between redox potential differences and rates of electron transfer between free flavin semiquinones and a series of homologous redox proteins.

It is interesting to note that although the FNR–rubredoxin system (Przysiecki et al., 1985) has a larger difference in redox potential ($\Delta E \sim 260$ mV) than the FNR–Fd system ($\Delta E \sim 50$ mV at pH 7.0), the rate of electron transfer from $FNR^{\bullet}$ to Rd_{ox} ($k = 2 \times 10^3$ s^{-1} at $I = 10$ mM) is at most half that observed for Fd_{red} to FNR_{ox} ($k = 4 \times 10^3$ s^{-1} at $I = 310$ mM; by extrapolation of the observed ionic strength effects, the k value should be even larger at $I = 10$ mM). This difference in rate constant magnitude could be a consequence of the relative distances and orientations of the participating redox centers within the electron-transfer complex. Thus, the electrostatic interactions in the nonphysiological FNR–Rd complex may not orient the two proteins in a manner as favorable to electron transfer as in the FNR–Fd complex, and the extent of structural reorganization that must occur prior to formation of the productive complex may be greater in the former than in the latter. This is consistent with the accessibility of the Fe center in the FNR–Rd complex being unchanged from that of free Rd (Przysiecki et al., 1985), whereas the Fe center is partially blocked in the FNR–Fd complex (see above).

The results obtained for the 1:1 complex at low ionic strength demonstrate that the FAD center in FNR remains exposed to solvent. On the basis of the structural homology between the Fd from *Spirulina platensis*, for which the three-dimensional structure is known (Tsukihara et al., 1981), and spinach Fd, there are two possible negatively charged FNR binding sites which occur on opposite sides of the Fd molecule. At present we cannot distinguish between these recognition sites, although it may be that both are being used simultaneously and that this accounts for the 2Fe-2S center being partially occluded due to FNR folding itself around the Fd molecule. When a high-resolution three-dimensional structure for FNR becomes available (Karplus & Herriott, 1982; Karplus et al., 1984), one may be able to generate hypothetical complexes by the use of computer graphics (Simondsen et al., 1982; Weber & Tollin, 1985) to test this possibility. We also have data (Bhattacharyya et al., 1986) on electron transfer and complex formation between FNR and some nonphysiological iron-containing high-potential electron acceptors (cytochromes, HiPIP's), which provide further information on the factors involved in determining the rate constants for electron transfer in electrostatic bimolecular complexes formed between two redox proteins.

Registry No. FNR, 9029-33-8; 5-dRf, 78548-68-2.

References

Ahmad, I., Cusanovich, M. A., & Tollin, G. (1982) *Biochemistry 21*, 3122–3128.

Batie, C. J., & Kamin, H. (1981) *J. Biol. Chem. 256*, 7756–7763.

Batie, C. H., & Kamin, H. (1984a) *J. Biol. Chem. 259*, 8832–8839.

Batie, C. J., & Kamin, H. (1984b) *J. Biol. Chem. 259*, 11976–11985.

Bhattacharyya, A. K., Tollin, G., Davis, M., & Edmondson, D. E. (1983) *Biochemistry 22*, 5270–5279.

Bhattacharyya, A. K., Tollin, G., McIntire, W., & Singer, T. P. (1985) *Biochem. J. 228*, 337–345.

Bhattacharyya, A. K., Meyer, T. E., Cusanovich, M. A., & Tollin, G. (1986) *Biochemistry* (submitted for publication).

Blankenhorn, G. (1976) *Eur. J. Biochem. 67*, 67–80.

Cusanovich, M. A., & Tollin, G. (1980) *Biochemistry 19*, 3343–3347.

Cusanovich, M. A., Meyer, T. E., & Tollin, G. (1985) *Biochemistry 24*, 1281–1287.

Draper, R. D., & Ingraham, L. L. (1968) *Arch. Biochem. Biophys. 125*, 802–808.

Foust, G. P., Mayhew, S. G., & Massey, V. (1969) *J. Biol. Chem. 244*, 964–970.

Hazzard, J. T., & Tollin, G. (1985) *Biochem. Biophys. Res. Commun. 130*, 1281–1286.

Hazzard, J. T., Cusanovich, M. A., Tainer, J. A., Getzoff, E. D., & Tollin, G. (1986) *Biochemistry 25*, 3318–3328.

Karplus, P. A., & Herriott, J. R. (1982) *Flavins Flavoproteins, Proc. Int. Symp., 6th*, 28–31.

Karplus, P. A., Walsh, K. A., & Herriott, J. R. (1984) *Biochemistry 23*, 6576–6583.

Keirns, J. J., & Wang, J. H. (1972) *J. Biol. Chem. 247*, 7374–7382.

Knaff, D. B., Smith, M. J., & Chain, R. K. (1980) *Arch. Biochem. Biophys. 199*, 117–122.

Masaki, R., Matsumoto, M., Yoshikawa, S. and Matsubara, H. (1982) in *Flavins Flavoproteins, Proc. Int. Symp., 6th*, 675–678.

Maskiewicz, R., & Bielski, H. J. B. (1982) *Biochim. Biophys. Acta 680*, 297–303.

Mayhew, S. G., Foust, G. P., & Massey, V. (1969) *J. Biol. Chem. 244*, 803–810.
Meyer, T. E., Przysiecki, C. T., Watkins, J. A., Bhattacharyya, A., Simondsen, R. P., Cusanovich, M. A., & Tollin, G. (1983) *Proc. Natl. Acad. Sci. U.S.A. 80*, 6740–6744.
O'Donnell, M. E., & Williams, C. H., Jr. (1983) *J. Biol. Chem. 258*, 13795–13805.
Ohnishi, T., King, T. E., Salerno, J. C., Blum, H., Bowyer, J. R., & Maida, T. (1981) *J. Biol. Chem. 256*, 5577–5582.
Przysiecki, C. T., Bhattacharyya, A. K., Tollin, G., & Cusanovich, M. A. (1985) *J. Biol. Chem. 260*, 1452–1458.
Shin, M., Sakihama, N., Nijmi, K., & Oshino, R. (1982) *Flavins Flavoproteins, Proc. Int. Symp., 6th*, 672–674.
Simondsen, R. P., & Tollin, G. (1983) *Biochemistry 22*, 3008–3016.
Simondsen, R. P., Weber, P. C., Salemme, F. R., & Tollin, G. (1982) *Biochemistry 21*, 6366–6375.
Smith, M. M., Smith, W. H., & Knaff, D. B. (1981a) *Biochim. Biophys. Acta 592*, 303–313.
Smith, M. M., Smith, W. H., & Knaff, D. B. (1981b) *Biochim. Biophys. Acta 635*, 405–411.
Stankovich, M. A., Schopfer, L. M., & Massey, V. (1978) *J. Biol. Chem. 253*, 4971–4979.
Stombaugh, N. A., Sundquist, J. E., & Orme-Johnson, W. J. (1976) *Biochemistry 15*, 2633–2641.
Tollin, G., Meyer, T. E., & Cusanovich, M. A. (1982) *Biochemistry 21*, 3849–3856.
Tsukihara, T., Fukuyama, K., Nakamura, M., Katsube, Y., Tanaka, N., Kakudo, M., Wada, K., Hase, T., & Matsubara, H. (1981) *J. Biochem. (Tokyo) 90*, 1763–1773.
Weber, P. C., & Tollin, G. (1985) *J. Biol. Chem. 260*, 5568–5573.
Zanetti, G., & Curti, B. (1980) *Methods Enzymol. 69*, 250–255.

Interaction of Spin-Labeled Nicotinamide Adenine Dinucleotide Phosphate with Chicken Liver Fatty Acid Synthase†

Soo-Ik Chang and Gordon G. Hammes*
Department of Chemistry, Cornell University, Ithaca, New York 14853-1301
Received February 5, 1986; Revised Manuscript Received April 10, 1986

ABSTRACT: The spatial relationships between the four reduced nicotinamide adenine dinucleotide phosphate (NADPH) binding sites on chicken liver fatty acid synthase were explored with electron paramagnetic resonance (EPR) and spin-labeled analogues of $NADP^+$. The analogues were prepared by reaction of $NADP^+$ with 2,2,5,5-tetramethyl-1-oxy-3-pyrroline-3-carboxylic acid, with 1,1′-carbonyldiimidazole as the coupling reagent. Several esterification products were characterized, and the interaction of the $N_{3'}$ ester of $NADP^+$ with the enzyme was examined in detail. Both $^1H_{13}$,^{14}N and $^2H_{13}$,^{15}N spin-labels were used: the EPR spectrum was simpler, and the sensitivity greater, for the latter. The spin-labeled $NADP^+$ is a competitive inhibitor of NADPH in fatty acid synthesis, and an EPR titration of the enzyme with the modified $NADP^+$ indicates four identical binding sites per enzyme molecule with a dissociation constant of 124 μM in 0.1 M potassium phosphate and 1 mM ethylenediaminetetraacetic acid (pH 7.0) at 25 °C. The EPR spectra indicate the bound spin-label is immobilized relative to the unbound probe. No evidence for electron–electron interactions between bound spin-labels was found with the native enzyme, the enzyme dissociated into monomers, or the enzyme with the enoyl reductase sites blocked by labeling the enzyme with pyridoxal 5′-phosphate. Furthermore, the EPR spectrum of bound ligand was the same in all cases. This indicates that the bound spin-labels are at least 15 Å apart, that the environment of the spin-label at all sites is similar, and that the environment is not altered by major structural changes in the enzyme. The EPR spectra were simulated with a stochastic Brownian motion model, and the rotational correlation times were found to be similar in the presence and absence of glycerol, indicating local rotation of the bound spin-label. The rotational correlation time at 25 °C is 27 ns, and its activation energy is 2.3 kcal/mol.

Animal fatty acid synthase is one of the most complex multienzyme complexes in the animal kingdom, and the molecular structure of the enzyme is not yet known. The chicken liver enzyme contains seven different enzyme activities and consists of two identical polypeptide chains per molecule [cf. Wakil et al. (1983)]. The structure of the chicken liver enzyme (M_r ~500 000) has been extensively probed with proteolytic enzymes (Wakil et al., 1983; Tsukamoto et al., 1983): the enzyme has three distinct structural domains. The dehydratase, the β-ketoacyl reductase, the enoyl reductase, and the 4′-phosphopantetheine are in one domain (M_r ~107 000). The other two structural domains contain the acetyl and malonyl transacylases (M_r ~127 000) and the thioesterase (M_r ~33 000), respectively. The β-ketoacyl synthase requires the interaction of two different structural domains, but the catalytic site is in the same structural domain as the transacylases.

The mechanism of action of the multienzyme complex involves initiation of the fatty acid chain by transfer of an acetyl group to the enzyme. The chain is then lengthened in two-carbon increments by the transfer of a malonyl residue to the enzyme. Each malonyl is condensed onto the growing chain (β-ketoacyl synthase); the resulting ketone is reduced to an

† This work was supported by grants from the National Institutes of Health (GM 13292) and the National Science Foundation (PCM 8120818).

0006-2960/86/0425-4661$01.50/0